Aggregation Behavior in Semidilute Rigid and Semirigid Polysaccharide Solutions

ARTICLE *in* MACROMOLECULES · MARCH 2002

Impact Factor: 5.8 · DOI: 10.1021/ma012047q

2 AUTHORS, INCLUDING:

Eric Buhler
Paris Diderot University
61 PUBLICATIONS **1,349** CITATIONS

SEE PROFILE

Aggregation Behavior in Semidilute Rigid and Semirigid Polysaccharide Solutions

Catherine Esquenet and Eric Buhler*

Centre de Recherches sur les Macromolécules Végétales, UPR No. 5301, CNRS, affiliated with Joseph Fourier University, BP53, 38041 Grenoble Cedex 9, France

Received November 26, 2001; Revised Manuscript Received February 5, 2002

ABSTRACT: Dynamic and static light scattering experiments were performed on 0.1 M NaCl aqueous solutions of semirigid hyaluronan and rigid xanthan in the dilute and semidilute regime. In the dilute regime, typical good solvent behavior is found, and the intrinsic persistence length of hyaluronan (≈100 Å) and xanthan (≈1000 Å) is determined. However, in the semidilute regime the time autocorrelation function of the scattered electric field is found to be bimodal for hyaluronan and xanthan solutions. The short time relaxation has a typical q^{-2} dependence and is attributed to the relaxation of concentration fluctuations characterized by a cooperative diffusion mechanism. The long time relaxation has a q^{-3} dependence, characteristic of intraparticle dynamics. This behavior is not consistent with predicted semidilute, good solvent system behavior but instead indicates the presence of associations or microgels. The corresponding slow relaxation times appear to be related to the macroscopic viscosity of the surrounding polymer solution. The effect of the molecular weight and polymer concentration was investigated.

Introduction

Over the past two decades water-soluble polyelectrolyte polysaccharides have been extensively studied for reasons of both scientific interest and commercial applications. Polysaccharides are natural polymers widely used in cosmetic, pharmaceutical, and food industries. In the present study, dynamic and static light scattering experiments were performed on aqueous solutions of hyaluronan (semirigid polymer) and xanthan (rigid polymer).

In solutions of polyelectrolytes, made from linear flexible polymers, an essential parameter is the polymer chain rigidity, which is strongly influenced by the ionic strength and in particular by the polyelectrolyte concentration. Electrostatic repulsions between charges along the chain will affect the local flexibility of the chain and will tend to increase the global size of the polyion. For semirigid polyelectrolytes the total persistence length, L_T, is written as[1]

$$L_T = L_0 + L_e \tag{1}$$

The total persistence length is the sum of two contributions: the intrinsic persistence length L_0 due to the rigidity of the uncharged chain and the electrostatic persistence length L_e arising from the repulsions between neighbor ionic sites. For polysaccharides the electrostatic contribution L_e is easily much smaller than the intrinsic contribution L_0. This is the reason why polysaccharides, in general, are called semirigid or rigid polymers. Several workers[1−4] have calculated the electrostatic contribution to the persistence length L_e. Odijk[1] and Skolnick and Fixman,[2] assuming a Debye−Hückel potential and if the condensation model applies,[5] have derived a formula giving L_e (if $\kappa L_T \gg 1$)

$$L_e = \frac{1}{4\kappa^2 l_B} \qquad \text{for } \lambda_0 \geq 1 \tag{2}$$

where l_B is the Bjerrum length ($l_B = e^2/\epsilon_0 kT = 7.13$ Å in water, ϵ_0 is the dielectric permittivity of the solvent, and e is the elementary charge) and κ^{-1} is the Debye−Hückel screening length related to the concentration of the counterions. $\lambda_0 = e^2/\epsilon_0 kTa$ (a being the distance between two ionic sites) is the structural charge parameter. For xanthan $\lambda_0 \sim 1$. For hyaluronan, the charge parameter is smaller than 1 ($\lambda_0 = 0.7$), and then L_e is given by

$$L_e = \frac{{\lambda_0}^2}{4\kappa^2 l_B} \qquad \text{for } \lambda_0 < 1 \tag{3}$$

with

$$\kappa^2 = 4\pi l_B c_f \tag{4}$$

In eq 4, c_f is the concentration of free monovalent ions ($c_f = c + 2c_s$ if $\lambda_0 < 1$ and $c/\lambda_0 + 2c_s$ if $\lambda_0 > 1$, where c is the polymer concentration and c_s the excess salt concentration). Since hyaluronan and xanthan have a larger intrinsic persistence length L_0 than the electrostatic persistence length L_e (at least for external salt concentration larger than 3×10^{-3} M), these polymers are characterized by a high rigidity, even in the high ionic strength solutions (κ^{-1} small).

In low-ionic-strength solutions we usually observe a slow polyelectrolyte mode in dilute and semidilute regime.[6−12] To avoid this slow polyelectrolyte mode, we have performed the experiments in large excess of salt ([NaCl] = 0.1 M) solutions, where the charged groups of the polyelectrolyte are screened by the salt ions. In this case the total persistence length L_T is equal to the intrinsic one L_0 (Debye screening length $\kappa^{-1} \approx 10$ Å and $L_e \approx 0$). In the present study, we will show that the studied systems are thermodynamically good (see section 3). Good solvent, semidilute systems in the presence of salt are not expected to display a slow mode behavior. However, in the present study, good solvent semirigid and rigid polysaccharide systems have been found to display slow mode behavior in the semidilute regime.

10.1021/ma012047q CCC: $22.00
Published on Web 03/28/2002

Table 1. Variation of the Radius of Gyration, of the Intrinsic Persistence Length, of the Hydrodynamic Radius, of the Second Virial Coefficient, of the Intrinsic Viscosity, and of the Overlap Concentration as a Function of the Hyaluronan and Xanthan Molecular Weight

sample	M_w (g/mol)	R_G (Å)	L_0 (Å)	R_H (Å)	$10^4 A_2$ (cm^3·mol/g^2)	$[\eta]$ (cm^3/g)	c^* (g/cm^3)
hyaluronan	85×10^3	270 ± 20	100	116 ± 10	9.5 ± 1.0	330 ± 50	3×10^{-3}
hyaluronan	610×10^3	600 ± 50	70	350 ± 30	6.0 ± 0.5	900 ± 100	1.1×10^{-3}
hyaluronan	900×10^3	760 ± 50	76	460 ± 40	5.3 ± 0.5	1200 ± 100	8.3×10^{-4}
hyaluronan	2×10^6	1200 ± 100	85	750 ± 70	4.3 ± 0.5	2500 ± 200	4×10^{-4}
xanthan	4.2×10^6		1020 ± 50		4.90[a]	1600 ± 200	6.25×10^{-4}

[a] Value obtained from ref 19; experiments performed at $\lambda = 633$ nm in the Guinier regime, i.e., $qR_G \ll 1$.

In the present paper, we report the effect of the high intrinsic rigidity, polymer concentration, and molecular weight on the structural and dynamical properties of dilute and semidilute good solvent polysaccharide solutions.

In section 2 of the paper, we describe materials and experimental techniques used in this study. In section 3, we report experimental results obtained from static and dynamic light scattering experiments in the dilute regime. These confirm the essentially ideal good solvent behavior of polysaccharide solutions. The intrinsic persistence length of semirigid hyaluronan and rigid xanthan is obtained. In section 4, we report combined light scattering and viscosity results obtained from aqueous hyaluronan and xanthan semidilute solutions and discuss these results. We show that the fast mode behavior is characteristic of typical, good solvent, semidilute behavior and that the slow mode behavior is due to polysaccharide associations or microgels.

2. Materials and Methods

2.1. Sample Characteristics. We have investigated aqueous solutions of 85×10^3, 610×10^3, 900×10^3, and 2×10^6 g/mol semirigid hyaluronan. Hyaluronan (HA) is a linear polysaccharide with the repeating disaccharide structure poly-[(1→3)-β-D-GlcNAc−(1→4)-β-D-GlcA]. Bacterial hyaluronan is produced by Soliance (Pomacle, France) and carefully purified under the Na salt form in our laboratory as described previously.[13] Hyaluronan belongs to a class of water-soluble polysaccharides, which can be called semirigid polyelectrolytes. Indeed, under conditions where the electrostatic repulsions are screened by addition of salt (0.1 M NaCl), it displays a large intrinsic persistence length L_0. The molar mass $M_w = 85$K was obtained by acid hydrolysis and determined by GPC. Also, the polydispersity was determined using GPC experiments and is equal to the ratio $M_w/M_n \approx 1.3$ (for 85K, 610K, and 900K HA samples and ≈1.4 for the 2×10^6 HA sample), where M_w is the weight-average molecular weight and M_n the number-average molecular weight. The mass of a monomer is equal to 400 g/mol, and the length of a monomer is equal to $a = 10.2$ Å. The aqueous solutions were investigated in the polymer concentration range from 10^{-4} to 10^{-2} g/cm^3 in the dilute and semidilute regime at the temperature $T = 25$ °C and in the presence of 0.1 M NaCl. Dilute and semidilute regime are separated by the critical overlap concentration c^*, i.e., when $c[\eta]$ is about unity. $[\eta]$ is the intrinsic viscosity of the solution and η the solution viscosity. Values of $[\eta]$ and of c^* for the different studied hyaluronan and xanthan samples are collected in Table 1. Also, the HA solutions were filtered through 0.2 μm Sartorius cellulose nitrate membranes. No aging effects were observed.

We have also investigated aqueous solutions of the 4.2×10^6 g/mol (polydispersity ≈ 1.4) rigid polysaccharide xanthan (produced by Aldrich and purified as usual) at 25 °C. Xanthan consists of a pentasaccharide repeating unit with a (1→4)-β-D-glucopyranan (cellulosic) backbone with *O*-β-D-mannopyranosyl-(1→4)-*O*-α-D-glucopyranosyluronic acid-(1→2)-6-*O*-acetyl-β-D-mannopyranosyl side chains 3-linked to alternate glucose residues. A pyruvic acetal substituent is present on the terminal mannose residue (39% determined by ^{1}H NMR).[14] The degree of acetate substitution is equal to 62%. The mass of a monomer is equal to 891 g/mol, and the length of a monomer is equal to $a = 10.3$ Å. There is still a question as to whether xanthan exists as a single or dimeric structure, and it is well-known that a conformational transition occurs with changes in ionic strength, pH, and temperature.[14,15] In the present study 0.1 M NaCl aqueous xanthan solutions were preheated before experiments in order to obtain an ordered conformation.[14,15] The polysaccharide is water-soluble and was dispersed in 0.1 M NaCl at room temperature by gentle shaking for 24 h. All samples were used within 6 days of preparation. Xanthan concentrations were prepared in the range 5×10^{-5}–3.5×10^{-3} g/cm^3. Prior to measurement the samples were filtered two times through a 3 μm Sartorius cellulose nitrate membrane and then through a 1.2 μm filter. The pore sizes being relatively large, we did not observe any effect of pore size on the profile of the correlation function. Also, very small amounts of xanthan derivative may be lost in the filters. The dilute solutions were directly very easily filtered through a 0.2 μm membrane.

2.2. Static Light Scattering. Static light scattering (SLS) and dynamic light scattering (DLS) experiments were performed by means of a spectrometer equipped with an argon ion laser (Spectra Physics model 2020) operating at $\lambda = 488$ nm, an ALV-5000 correlator (ALV, Langen-Germany Instruments), a computer-controlled and stepping-motor-driven variable angle detection system, and a temperature-controlled sample cell. Temperature was 25 ± 0.1 °C unless otherwise noted. The scattering spectrum was measured through a band-pass filter (488 nm) and a pinhole (200 μm for the static experiments and 100 or 50 μm for the dynamic experiments) with a photomultiplier tube (ALV).

In the SLS experiments, the excess of scattered intensity $I(q)$ was measured with respect to the solvent, where the magnitude of the scattering wave vector q is given by

$$q = \frac{4\pi n}{\lambda} \sin \frac{\theta}{2} \tag{5}$$

In eq 5, n is the refractive index of the solvent (1.34 for the water at 25 °C), λ is the wavelength of light in the vacuum, and θ is the scattering angle. In our experiments, the scattering angle θ was varied between 20° and 150°, which corresponds to scattering wave vectors q in the range from 6×10^{-4} to 3.2×10^{-3} Å^{-1}. The absolute scattering intensities $I(q)$ (i.e., the excess Rayleigh ratio) were deduced by using a toluene sample reference for which the Rayleigh ratio is well-known, i.e., 40×10^{-6} cm^{-1} at 488 nm.

A virial expression for the osmotic pressure can be used in dilute regime to deduce the following relationship:

$$\frac{Kc}{I(q,c)} = \frac{1}{M_w}\left[1 + q^2 \frac{R_G^2}{3} + ...\right] + 2A_2 Q(q,c)c + ... \tag{6}$$

The function $Q(q,c)$ is approximately unity for flexible polymer chains, but not for spheres;[16] $Q(0,c)$ is equal to 1 in any case. c is the polymer concentration, and A_2 is the second virial coefficient, which describes the polymer−solvent interactions. The scattering constant is $K = 4\pi^2 n^2 (dn/dc)^2 / N_A \lambda^4$, where dn/dc is the refractive index increment and N_A is Avogadro's number. The dn/dc of xanthan[14] and hyaluronan[13] in 0.1 M NaCl aqueous solutions is equal to 0.143 and 0.14 cm^3/g,

respectively. The plots of $c/I(q,c)$ vs q^2 were extrapolated to $q = 0$ to give intercepts $c/I(0,c)$. If the length scale q^{-1} is sufficiently large compared to the radius of gyration R_G of the polymers, the form factor obeys Guinier's law, and the apparent radius of gyration $R_{G,app}$ can be determined from the intercept and the initial slope of these plots using a scattering inverse Lorentzian law of the form[16]

$$\frac{c}{I(q,c)} = \frac{c}{I(0,c)}\left[1 + \frac{q^2 R_{G,app}{}^2}{3}\right] \qquad \text{if } qR_G \ll 1 \tag{7}$$

The weight-average molecular weight[16] M_w can be obtained from

$$\frac{I(0,c)}{Kc} = M_{w,app} = M_w(1 - 2A_2M_wc) \tag{8}$$

The apparent mass $M_{w,app}$ of polymers in solution at a concentration c is given by extrapolation of the scattered intensity $I(q)/c$ to $q = 0$, while the apparent radius of gyration is obtained by a mean-square linear fit of the inverse of the scattered intensity vs q^2.

2.3. Dynamic Light Scattering. In the dynamic light scattering experiments (DLS), the normalized time autocorrelation function $g^{(2)}(q,t)$ of the scattered intensity is measured.[16]

$$g^{(2)}(q,t) = \frac{\langle I(q,0)\, I(q,t)\rangle}{\langle I(q,0)\rangle^2} \tag{9}$$

The latter can be expressed in terms of the field autocorrelation function or equivalently in terms of the autocorrelation function of the concentration fluctuations $g^{(1)}(q,t)$ through

$$g^{(2)}(q,t) = A + \beta|g^{(1)}(q,t)|^2 \tag{10}$$

where A is the baseline and β is the coherence factor which in our experiments is equal to 0.7−0.9. The normalized dynamical correlation function $g^{(1)}(q,t)$ of polymer concentration fluctuations is defined as

$$g^{(1)}(q,t) = \frac{\langle \delta c(q,0)\, \delta c(q,t)\rangle}{\langle \delta c(q,0)^2\rangle} \tag{11}$$

where $\delta c(q,t)$ and $\delta c(q,0)$ represent fluctuations of polymer concentration at time t and zero, respectively.

In our experiments, the inspection of the angular dependence shows that some relaxations are diffusive with characteristic time inversely proportioned to q^2. Dilute polymer solutions were characterized by a single relaxation mechanism. For these solutions (if the relaxation is diffusive) we have adopted the classical cumulant analysis.[17] This analysis provides the variance of the correlation function and the first reduced cumulant $(\tau q^2)^{-1}$, where τ is the average relaxation time of $g^{(1)}(q,t)$. The extrapolation of $(\tau q^2)^{-1}$ to $q = 0$ yields the values of the mutual diffusion constant D. The latter is related to the average hydrodynamic radius R_H of the macromolecules through

$$D = \frac{kT}{6\pi\eta_s R_H} = \left(\frac{1}{\tau q^2}\right)_{q^2=0} \tag{12}$$

where k is the Boltzmann constant, η_s the solvent viscosity, and T the absolute temperature.

We also used another method to determine the average relaxation time τ: the Contin method based on the inverse Laplace transform of $g^{(1)}(q,t)$.[18] If the spectral profile of the scattered light can be described by a multi-Lorentzian curve, then $g^{(1)}(q,t)$ can be written as

$$g^{(1)}(q,t) = \int_0^\infty G(\Gamma)\exp(-\Gamma t)\, d\Gamma \tag{13}$$

where $G(\Gamma)$ is the normalized decay constant distribution. This method is more appropriate for the solutions characterized by several relaxation mechanisms (i.e., semidilute solutions).

2.4. Viscosity Measurements. The viscosity measurements were carried out by using a low-shear 40 coaxial viscometer, on the Newtonian plateau, within the range of polymer concentration from 10^{-4} to 4×10^{-3} g/cm^3, which is the same as for the light scattering experiments.

3. Results and Discussion: Dilute Regime

3.1. Dilute Semirigid Polymer Solutions: Case of Hyaluronan. For the dilute hyaluronan solutions, the radius of gyration R_G and the second virial coefficient A_2 can be determined from the static light scattering experiments using eq 6. Values of R_G and A_2 for the four studied hyaluronan molecular weight samples are collected in Table 1. The experimental results indicate that dilute, aqueous solutions of hyaluronan and xanthan exhibit typical good solvent behavior with a positive second virial coefficient (see Table 1).[19] For hyaluronan dilute solutions, we have

$$A_2 = 0.0155 M_w{}^{-0.25}\ \text{cm}^3\cdot\text{mol/g}^2 \tag{14}$$

This scaling law confirms the good solvent behavior of hyaluronan dilute solutions.[20] Actually, the theoretical power law[20] dependence for monodisperse random coil polymers in a good solvent is $A_2 \propto M_w{}^{-0.20}$. Also, the experimental value of the exponent is in very good agreement with the value obtained in many other good solvent systems.[21]

Benoît and Doty[22] have used the persistence length L_T and the contour length L_c to calculate the unperturbed radius of gyration $R_G{}^2$ (screening of the electrostatic repulsions by salt addition). In this case, we are neglecting the interactions between macromolecules.

$$\langle R_G{}^2\rangle = \frac{L_cL_T}{3} - L_T{}^2 + 2\frac{L_T{}^3}{L_c} - 2\frac{L_T{}^4}{L_c{}^2}\left[1 - \exp\left(\frac{-L_c}{L_T}\right)\right] \tag{15}$$

This is the basis of the "wormlike chain" model and serves as a bridge between the rod limit where $L_T \gg L_c$ and $R_G{}^2 = L_c{}^2/12$ and the random coil limit where $L_c \gg L_T$ and $R_G{}^2 = L_cL_T/3$. The intrinsic persistence length $L_0 \approx L_T = 3R_G{}^2/L_c$ could be obtained from the value of the radius of gyration. The electrostatic repulsions being screened ($\kappa^{-1} \approx 10$ Å and $L_e \approx 0$), the total persistence length L_T is approximately equal to the intrinsic one L_0. L_e is close from 0 according to eq 3. Values of L_0 obtained for the four studied hyaluronan molecular weight samples are collected in Table 1. In this case we are neglecting the polydispersity effect. These values are in very good agreement with the value $L_0 = 86$ Å obtained from small-angle neutron scattering experiments performed on 0.1 M NaCl aqueous solutions of hyaluronan.[23]

Also for the DLS data in the dilute regime, the normalized field autocorrelation function $g^{(1)}(q,t)$ is found to be characterized by a simple exponential relaxation (see Figure 1). The fitted curve to the correlation function obtained with a single exponential expression is also presented in Figure 1. Also, note that the cumulant method (method used) and the Contin method are in good agreement. The angular dependence shows that this relaxation is diffusive with a characteristic time inversely proportioned to q^2. The diffusion

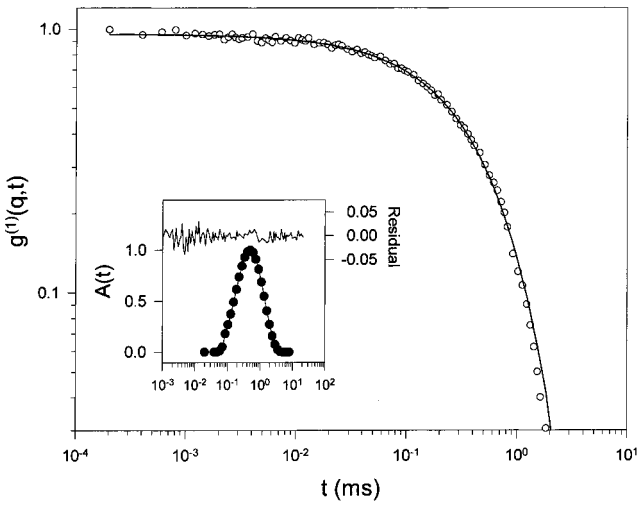

Figure 1. A log−log representation of $g^{(1)}(q,t)$ for $\theta = 90°$ relative to a dilute 900K hyaluronan solution at polymer concentration $c = 3 \times 10^{-4}$ g/cm^3. The inset represents the distribution function of decay times $A(t)$ obtained using the Contin method. The black line represents the fit of $g^{(1)}(q,t)$ obtained using a simple monoexponential expression. The residual plot of this fitting procedure is also presented in the inset.

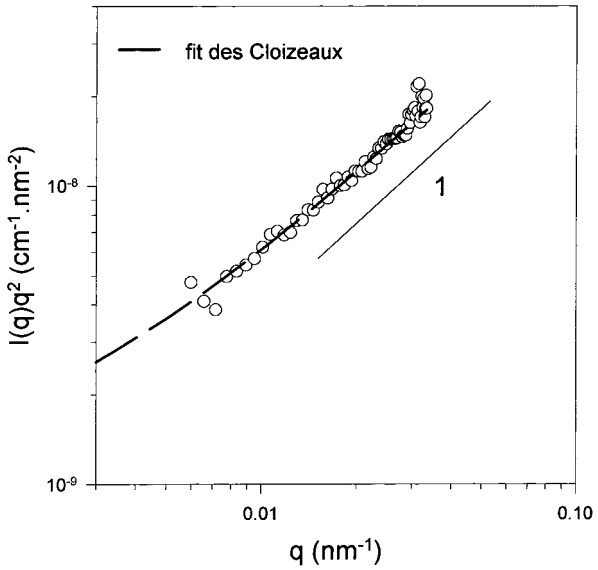

Figure 2. Variation of Iq^2 with q measured in xanthan dilute solution at polymer concentration $c = 10^{-4}$ g/cm^3. The dashed line represents the des Cloizeaux fit.

coefficient and the hydrodynamic radius of the hyaluronan chain are obtained (cf. eq 12). Values of R_H for the four studied hyaluronan samples are also collected in Table 1. The inspection of the molecular weight dependencies of various quantities reveals that $R_G \sim M_w^{0.5}$, $R_H \sim M_w^{0.6}$, and $[\eta] \sim M_w^{0.83}$. These data are in rather good agreement with the theoretical predictions in good solvent,[20] i.e., $R \sim M^{3/5}$ and $[\eta] \sim M^{4/5}$.

3.2. Dilute Rigid Polymer Solutions: Case of Xanthan. There is a crossover in the scattering curve intensity, $I(q)$, as a function of the scattering wave vector q in the q range where the transition between the asymptotic regime of a coil and a rod occurs. In the first case the form factor $P(q)$ is q^{-2}-dependent, whereas when we look at smaller distances than L_T the form factor is q^{-1}-dependent. One usually uses a Kratky plot[24] to represent the experimental curves. In such a plot we represent the product $I(q)q^2$ as a function of q as it is shown in Figure 2. The value of L_T could be extracted by fitting the curve to the Sharp−Bloomfield[25] scattering form factor $P(q)$ of a single finite monodisperse wormlike chain of contour length L_c

$$P(q) = \frac{2[\exp(-x) + x - 1]}{x^2} + \left[\frac{4}{15} + \frac{7}{15x} - \left(\frac{11}{15} + \frac{7}{15x}\right)\exp(-x)\right]\frac{2L_T}{L_c} \quad (16)$$

with $x = L_c L_T q^2/3$. It is an approximation, which is only valid for $L_c > 10L_T$ in a q range $qL_T < 2$. For $qL_T = 2$, the values overlap[26] the curve rigorously obtained by des Cloizeaux[27] for chains of infinite length, which will be used for $qL_T > 2$:

$$P(q) = \frac{\pi}{qL_c} + \frac{2}{3q^2 L_T L_c} \quad (17)$$

The L_T value should be obtained by fitting the data in the whole q range with simultaneously the Sharp−Bloomfield equation ($qL_T < 2$) and the des Cloizeaux equation ($qL_T > 2$). The equations are characterized by two parameters: the persistence length L_T and the contour length $L_c = Na$.

At low xanthan concentration, in the dilute regime, the representation of $q^2I(q)$ as a function of q given in Figure 2 shows that, for wavevectors q investigated by SLS, $I(q)$ is q^{-1}-dependent. This suggests that xanthan chains are locally rigid over a persistence length $L_0 \approx L_T$. The experimental light scattering curves are fitted with the wormlike chain model[26] and assuming $I(q) \approx KcM_wP(q)$, i.e., neglecting the interactions between macromolecules (electrostatic repulsions are screened by salt addition, $\kappa^{-1} \approx 10$ Å). In this model the chain is rodlike for small scales and follows a random walk to large scales. The two parameters L_0 and $M_L = M_w/L_c$ may be obtained from the fit of the data using the asymptotic expression derived by des Cloizeaux[27] (chains of infinite length, see eq 17). The fit is performed using a representation $q^2I(q)$ vs q. For xanthan one obtains $L_0 = 1020 \pm 50$ Å and $M_L = M_w/L_c = 240 \pm 50$ g mol^{-1}/Å depending on the polymer concentration ($L_c \gg L_0$). These values are in very good agreement with the values obtained by Stokke and al.[15] using electron microscopy experiments. According to the value of M_L, the authors proposed a double-stranded conformation for xanthan. Also, the evaluation of the persistence length of xanthan[28] considering the polydispersity of the sample was already determined[29] as well as xanthan second virial coefficient as a function of the molecular weight[28,30,31] in the same medium of the present work.

In the dilute regime, the autocorrelation function of the scattered electric field $g^{(1)}(q,t)$ is a single relaxation. The peak in the time distribution function obtained using the Contin procedure shows a dissymmetry, as would be the case for a stretched exponential relaxation mode. A good quality of fit can be obtained using a stretched exponential with an exponent γ varying between 0.65 and 0.75 depending on the scattering wavevector. Also, the characteristic relaxation time is characterized by a q^{-3} dependence (see Figure 3). One must also note that, since the polymer chain size is larger than the q^{-1} range explored according to Figure 2, the relaxation of the index fluctuations should be due

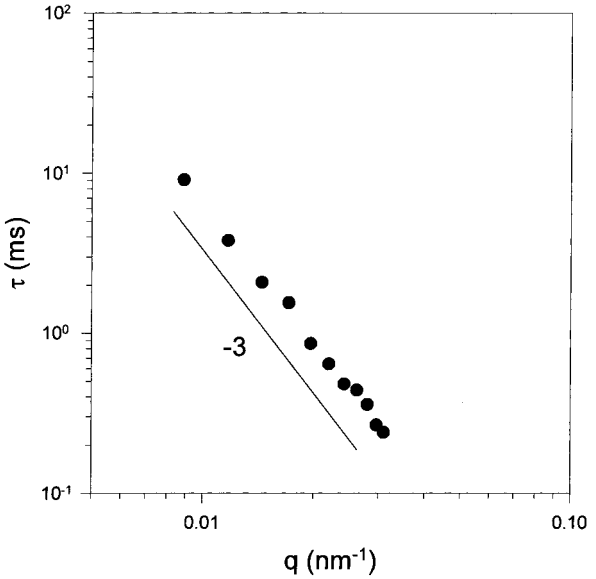

Figure 3. Variation of the characteristic relaxation time τ with q measured in xanthan dilute solution at polymer concentration $c = 10^{-4}$ g/cm^3.

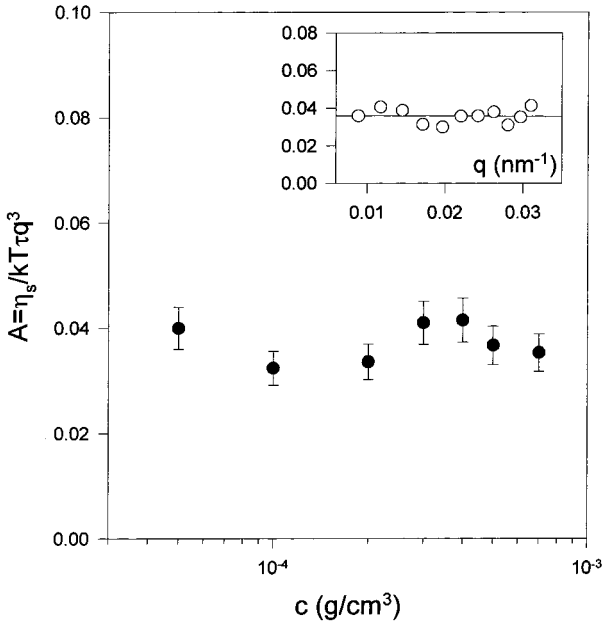

Figure 4. Variation of $A = \eta_s/kT\tau q^3$ with the xanthan concentration in the dilute regime. The inset represents A vs q for $c = 5 \times 10^{-5}$ g/cm^3.

to internal modes of the xanthan chains, as long as the latter are not compact. One can show that, in the case of linear polymers, the q^{-3} dependence of characteristic times corresponding to internal modes comes with a stretched exponential relaxation function having an exponent $\gamma = {}^2/_3$.[32−34] The experimental values of γ in the whole investigated q range are close to that value. Furthermore, the characteristic decay time of the scattering function was predicted to vary like

$$\tau^{-1} = A \frac{kT}{\eta_s} q^3 \qquad (18)$$

where η_s is the viscosity of the solvent, τ^{-1} is the inverse first cumulant of the field autocorrelation function, and A is a numerical constant that depends on the quality of the solvent;[35] $A \approx 0.08$ according to an approach based on the linear response theory, whereas the renormalization group calculation led to $A \approx 0.045$. Figure 4 shows the dependence of the quantity $\eta_s/kT\tau q^3$ with the xanthan concentration in the dilute regime. In the whole q range (see inset in Figure 4) and concentration range, the data tend to a plateau around 0.04. The high rigidity of xanthan could explain a lower value than 0.045 for A.

4. Semidilute Semirigid and Rigid Polymer Solutions

4.1. Dynamic Light Scattering. The separation between dilute and semidilute regime is characterized by the critical overlap concentration c^*, i.e., when $c[\eta]$ is about unity.[20] $[\eta]$ is the intrinsic viscosity of the solution and η the solution viscosity. Values of $[\eta]$ and c^* for the different studied hyaluronan and xanthan samples are collected in Table 1.

Parts a and b of Figure 5 show a typical correlation function $g^{(1)}(q,t)$ obtained for semidilute aqueous solutions of hyaluronan and xanthan, respectively. The inset shows the normalized time distribution function $A(t)$ obtained using the Contin method. The DLS results suggest two well-defined characteristic times for the relaxation function $g^{(1)}(q,t)$. The peak in time distribution function corresponding to the fast mode is quite symmetric as expected for a simple exponential relaxation, while the slow mode shows a dissymmetry (for high hyaluronan molecular weight samples and for xanthan samples) as would be the case for a stretched exponential relaxation mode (see Figure 5b). To analyze the quasi-elastic light scattering data within this context, the scattered electric field time autocorrelation function $g^{(1)}(q,t)$ was fitted using the following general form:

$$g^{(1)}(q,t) = A_{\text{fast}}(q)\mathrm{e}^{-(t/\tau_{\text{fast}})} + A_{\text{slow}}(q)\mathrm{e}^{-(t/\tau_{\text{slow}})^{\gamma}} \qquad (19)$$

with $A_{\text{fast}}(q) + A_{\text{slow}}(q) = 1$. τ_{fast} and τ_{slow} are respectively the fast and the slow characteristic relaxation time. $A_{\text{fast}}(q)$ and $A_{\text{slow}}(q)$ are the corresponding amplitudes. $\gamma = 1$ for the low hyaluronan molecular weight samples (M_w = 85K, 610K, and 900K), and $\gamma \approx {}^2/_3$ for the high hyaluronan molecular weight samples ($M_w = 2 \times 10^6$) and xanthan samples. The Contin method was used as a diagnostic tool to indicate the number of relaxation modes and to determine $A_{\text{fast}}(q)$ and $A_{\text{slow}}(q)$. Values of A_{fast} and A_{slow} determined using the Contin method and eq 19 are in very good agreement. $\tau_{\text{fast}}(q)$, $\tau_{\text{slow}}(q)$, and γ were obtained by fitting the correlation function with the sum of a single exponential and a stretched exponential (see eq 19). Then mean relaxation times were calculated. γ is varying between 0.59 and 0.67 depending on the scattering wavevector and on the polymer concentration. The fitted curves to the correlation function (with eq 19) are presented in Figure 5a,b, and the goodness of the fitting procedure is illustrated in form of residual plots (see inset). If $\gamma = 1$, the two relaxation modes being well separated in time, the classical Contin method was used. A good agreement is found with the fit obtained using eq 19.

The inspection of Figure 6, representing the variation of τ_{fast} and τ_{slow} with q for a xanthan solution at a polymer concentration equal to 2×10^{-3} g/cm^3 and a 900K hyaluronan solution at $c = 5 \times 10^{-3}$ g/cm^3 (asymptotic semidilute regime), shows clearly that the fast mode is diffusive with a characteristic time τ_{fast}

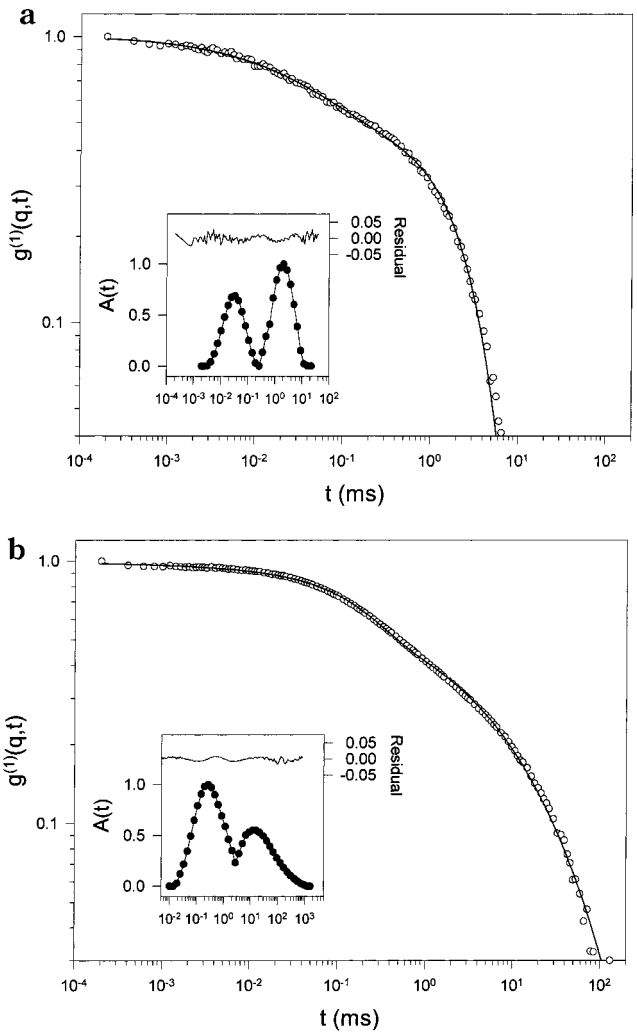

Figure 5. (a) A log−log representation of $g^{(1)}(q,t)$ for $\theta = 130°$ relative to a 900K hyaluronan semidilute solution at polymer concentration $c = 5 \times 10^{-3}$ g/cm^3. The peaks in time distribution function corresponding to the fast and the slow mode are quite symmetric (see inset). For low hyaluronan molecular weight samples (85K, 610K, and 900K), the slow relaxation time presents a q^{-2} dependence and $\gamma = 1$. The black line represents the fit of $g^{(1)}(q,t)$ obtained using eq 19. The residual plot of this fit is also presented in the inset. (b) A log−log representation of $g^{(1)}(q,t)$ for $\theta = 130°$ relative to a xanthan semidilute solution at polymer concentration $c = 2 \times 10^{-3}$ g/cm^3. The peak corresponding to the slow mode shows a dissymmetry (see inset) as would be the case for a stretched exponential relaxation mode. In this case τ_{slow} is q^{-3}-dependent and $\gamma = 0.67$. The black line represents the fit of $g^{(1)}(q,t)$ obtained using eq 19. The residual plot of this fit is also presented in the inset.

inversely proportioned to q^2. Thus, it is possible to calculate for each polymer concentration a fast diffusion coefficient D. For xanthan and high hyaluronan molecular weight solutions ($\gamma \approx {}^2/_3$), slow relaxation times, τ_{slow}, are characterized by a q^{-3} dependence. However, for low hyaluronan molecular weigth samples ($\gamma = 1$), the slow relaxation time presents a q^{-2} dependence (see Figure 6).

It is worth noting that in fact the corresponding amplitudes are dependent on the scattering wave vector q, as shown in Figure 7. Figure 7a shows the q dependence of the ratio A_{slow}/A_{fast} for different xanthan concentrations. The variation of A_{slow}/A_{fast} at $q = 0$ with the xanthan and the 900K hyaluronan concentration can be observed in Figure 7b. Figure 8 shows the

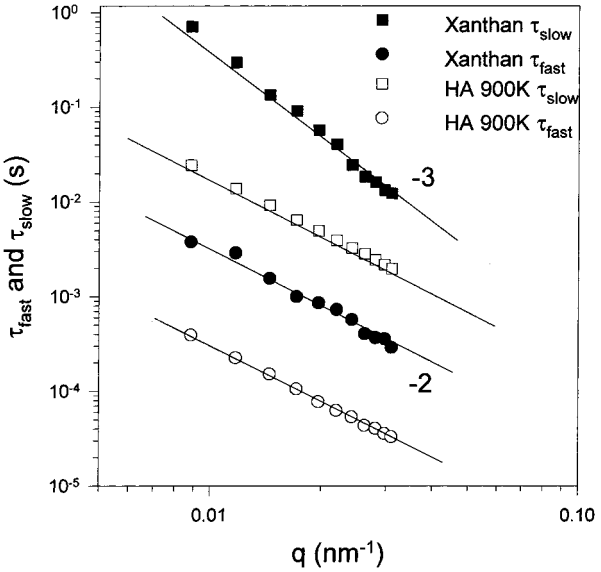

Figure 6. Variation of the fast characteristic time and of the slow characteristic time with q measured in $c = 2 \times 10^{-3}$ g/cm^3 xanthan and $c = 5 \times 10^{-3}$ g/cm^3 900K hyaluronan semidilute solutions.

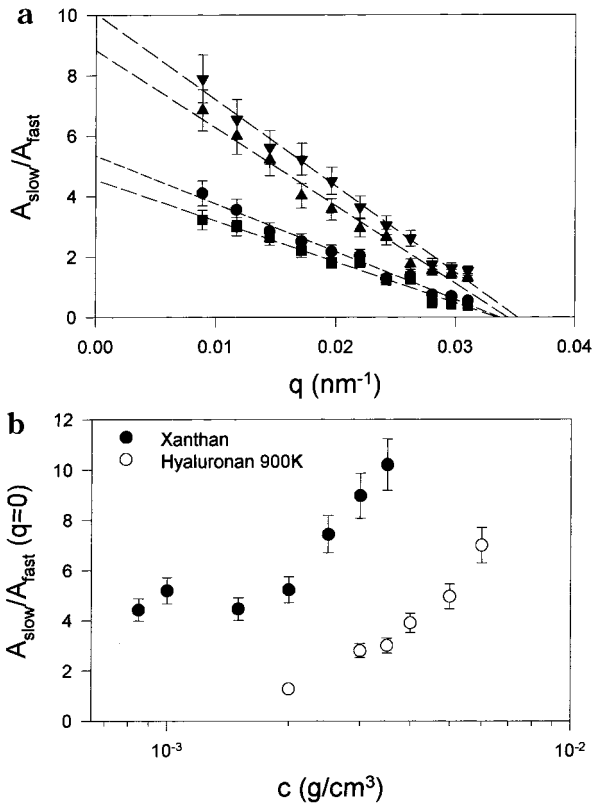

Figure 7. Scattering wavevector dependence (a) of A_{slow}/A_{fast} for xanthan solutions at $c = 1.5 \times 10^{-3}$ g/cm^3 (■), $c = 2 \times 10^{-3}$ g/cm^3 (●), $c = 3 \times 10^{-3}$ g/cm^3 (▲), and $c = 3.5 \times 10^{-3}$ g/cm^3 (▼). (b) Xanthan (●) and 900K hyaluronan (○) concentration dependence of A_{slow}/A_{fast} at $q = 0$. The dashed line represents the fit of the data.

increase of the scattered intensity extrapolated to zero wavevector with the increase of the xanthan and the 900K hyaluronan concentration. Note that similar results are observed with hyaluronan and xanthan solutions.

4.2. Fast Relaxation Mode. In the semidilute asymptotic regime, the fast diffusion coefficient, D, derived

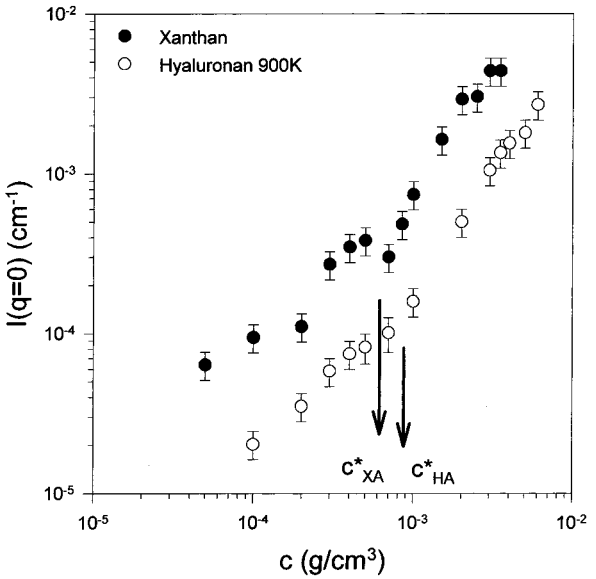

Figure 8. Light scattering intensity at zero angle as a function of the xanthan (●) and 900K hyaluronan (○) concentration. The arrows indicate the critical overlap concentrations c^*.

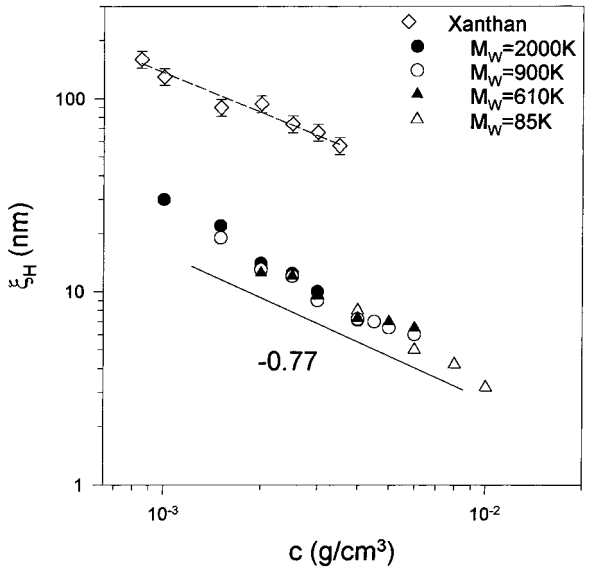

Figure 9. Dependence of the hydrodynamic correlation length on the hyaluronan concentration for four molecular weights: 85K (△), 610K (▲), 900K (○), and 2×10^6 (●). $\xi_H \propto c^{-0.80}$, $\xi_H \propto c^{-0.65}$, $\xi_H \propto c^{-0.86}$, and $\xi_H \propto c^{-0.94}$ for hyaluronan molecular weight equal to 85K, 610K, 900K, and 2×10^6, respectively. The experimental error is equal to 10%. (◇) Dependence of the hydrodynamic correlation length on the xanthan concentration; the dashed line represents the fit of the data: $\xi_H \propto c^{-0.68}$.

from the fast relaxation increases consequently with polymer concentration. In this regime, the variation of the coefficient diffusion with polymer (hyaluronan and xanthan) concentration can be described by a power law characterized by an exponent close from 0.77. de Gennes developed a scaling theory for semidilute solutions in thermodynamically good solvents.[20] The main prediction of this theory is that the dynamical behavior of the solution can be described in terms of a single characteristic length, that is, the correlation length ξ. Then the cooperative diffusion coefficient D is given by

$$D = \frac{kT}{6\pi\eta_s\xi_H} \tag{20}$$

where ξ_H is the hydrodynamic correlation length that scales like the static correlation length ξ. The correlation length of concentration fluctuations (often described as a mesh size), which is predicted to be molecular weight independent, and consequently the cooperative diffusion coefficient D follow simple scaling laws to dilution according to[20]

$$\xi \approx c^{-0.77} \quad \text{and} \quad D \approx c^{0.77} \tag{21}$$

Values of ξ_H as a function of the hyaluronan and xanthan concentration are plotted in Figure 9. Figure 9 shows the independence of the correlation length on the hyaluronan molecular weight. Note that the variation of ξ_H with the xanthan concentration requires care because the mesh size of the xanthan semidilute network is smaller than the persistence length L_0 for the high polymer concentrations.

4.3. Slow Relaxation Process. The presence of a slow mode is not an uncommon feature and has been observed in many different systems including low ionic strength polyelectrolyte solutions,[11,12] high ionic strength polyelectrolyte solutions,[36,37] associating polymer solutions,[38,39] linear neutral polymer systems in good[40] and in Θ solvents,[41] and nearly all classes of charged macromolecular systems in dilute and in concentrate solutions. Although the generic name of slow mode is widely used, its physical origin may differ according to the considered system. In particular, dynamic coupling of elementary processes, coupling of stress and polymer concentration fluctuations,[40] and diffusion of large particle aggregates[36,37] or of polymer domains[11] are possible mechanisms that might be responsible for a slow component in the time autocorrelation function of the scattered electric field. However, in the present study the slow mode appears only for polymer concentrations larger than the overlap concentration c^*, the dilute solutions showing a classical good solvent behavior. Moreover, our experiments were carried out under high-ionic-strength polyelectrolyte solutions where long-range electrostatic interactions are certainly screened (excess salt concentration equal to 0.1 M).

In the present case we have showed that the slow amplitude, A_{slow}, and the slow relaxation time, τ_{slow}, are q-dependent. In fact, in the semidilute regime, the network is deformed when fluctuations of polymer concentration are relaxing cooperatively.[40,42−45] This network deformation is responsible for a local stress fluctuation relaxing on a much longer time scale. The amplitude of this viscoelastic relaxation is directly related to the ratio of the elastic and osmotic modulus.[42] However, an experimental study of Buhler et al.[40] and detailed derivations of this model[43−45] show no q dependence for the slow viscoelastic relaxation time and for the associated slow relative amplitude, contrary to our results. Moreover, the increase of A_{slow} and of the scattered intensity (see Figures 7 and 8) with polymer concentration and the increase of A_{slow} with the decrease of q suggest that the slow mode is due to the formation of aggregates, associations, or domains. The pronounced q dependence of A_{slow} is due to the formation of association complexes, and then an enhanced effect is observed at higher concentrations.

The $\tau_{slow} \approx q^{-3}$ behavior observed with high hyaluronan molecular weight samples and xanthan samples is

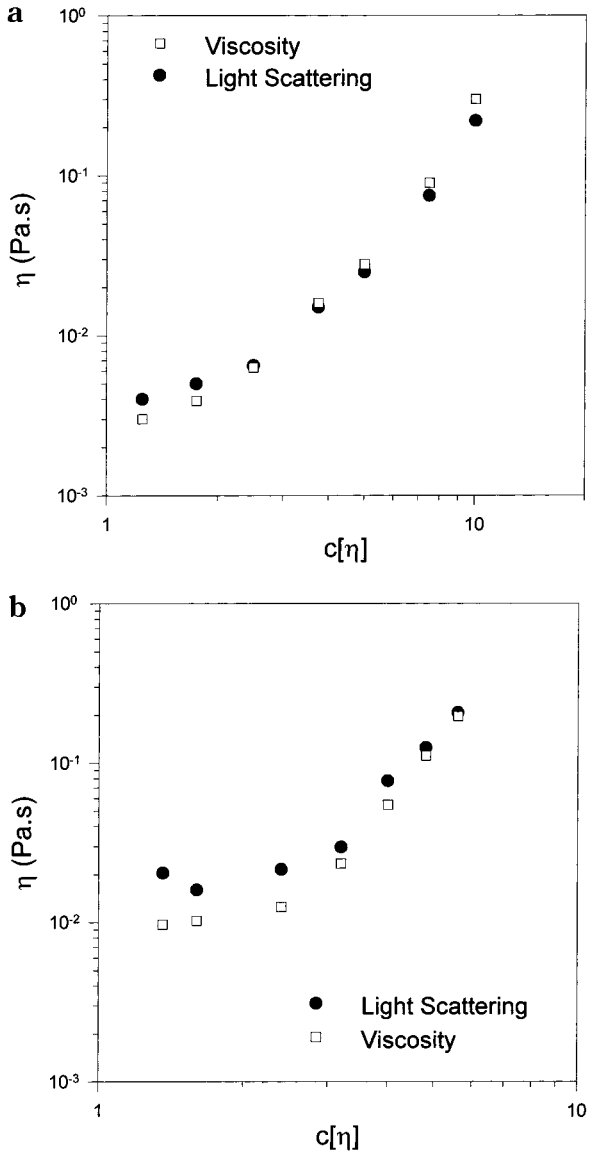

Figure 10. (a) Dependence on $c[\eta]$ of the hyaluronan solution viscosity calculated (●) using eq 22 and assuming $A = (6\pi)^{-1}$ and of the measured solution viscosity (□) in the semidilute regime. The molecular weight is equal to 2×10^6 g/mol, and the experimental error is equal to 10%. (b) Dependence on $c[\eta]$ of the xanthan solution viscosity calculated (●) using eq 22 and assuming $A = 0.04$ and of the measured solution viscosity (□). The experimental error is equal to 10%.

consistent with internal modes dynamics.[32−35] The slowly fluctuating intensity could originate from a texture or domain whose characteristic length would be much larger than the largest q^{-1} value explored in the light scattering experiments, i.e., much larger than 200 nm. In analogy with dilute solutions of long polymers,[33,35] we would write

$$\tau_{\text{slow}}{}^{-1} = A\frac{kT}{\eta}q^3 \qquad (22)$$

where η is a viscosity and A a numerical constant. If large objects (polymer associations) are immersed in a semidilute solution, the viscosity η should tend to equal the macroscopic viscosity, i.e., the solution viscosity. Figure 10 shows η values calculated from the experimental $\tau_{\text{slow}}(q)$ values using eq 22 and assuming arbitrarily $A = (6\pi)^{-1}$ for hyaluronan data (Figure 10a) and $A = 0.04$ for xanthan data (according to the dilute xanthan solutions results; Figure 10b) as a function of $c[\eta]$. In Figure 10 is also plotted the measured solution viscosity, and an excellent agreement is found between the two sets of viscosity. This result suggests that the characteristic time of the slow relaxation is in some way linked to the macroscopic viscosity of the underlying semidilute solution.

For low hyaluronan molecular weight samples (M_w = 85K, 610K, and 900K) the slow relaxation time presents a q^{-2} dependence, characteristic of the cooperative diffusion mechanism of the polymer associations. If q^{-1} is larger than the size of these associations, it is possible to determine an apparent radius of gyration of these domains responsible for the slow component. The apparent radius of gyration of the aggregates $(R_G)_{\text{slow,app}}$ was determined using the following relation:

$$I_{\text{slow}}(q,c_{\text{slow}}) = I_{\text{slow}}(0,c_{\text{slow}})\left[1 - \frac{1}{3}q^2(R_G{}^2)_{\text{slow,app}}\right] \quad \text{if } q(R_G)_{\text{slow,app}} \ll 1 \qquad (23)$$

where $I_{\text{slow}}(q) = A_{\text{slow}}(q)I(q)$ is the slow scattered intensity and c_{slow} the concentration of aggregates. Data reveal $(R_G)_{\text{slow,app}}$ values of 170 ± 20 nm over the whole 900K hyaluronan semidilute concentration range. $(R_G)_{\text{slow,app}} = 130 \pm 20$ nm and $(R_G)_{\text{slow,app}} = 50 \pm 20$ nm for hyaluronan molecular weight equal to 610K and 85K, respectively. The dimensions of these associations increase with increasing the molecular weight and become larger than q^{-1}. τ_{slow} becomes then q^{-3}-dependent ($M_w = 2 \times 10^6$ g/mol). Also, for the low-molecular-weight samples, we are expected a transition to a q^{-3} dependence of the slow mode at higher concentrations due to the formation of large association complexes. However, in the investigated concentration range, we have observed no transition.

A slow mode corresponding to polymer associations is essentially not observed with solutions in good solvents but rather requires a solution under Θ conditions with $A_2 \approx 0$ to be a dominant effect. A slow polyelectrolyte mode is also usually observed in low-ionic-strength solutions. Is the high intrinsic rigidity of hyaluronan and xanthan related to some state of physical polymer associations in semidilute regime? It would be interesting to investigate in more detail the role of hydrogen bonding in these polysaccharide solutions along the same lines as Sun and King.[46] The role of hydrogen bonding in the association process should be studied. However, the nature of these associations still remains an open question. Such aggregates seem to be a general feature of many charged polysaccharides.[47−51] Associations can be formed, for example, as a result of lateral arrangement of segments of different macromolecules. Such aggregates were recently proposed for some derivatives of another polysaccharide, cellulose.[48] Other studies have also shown the apparition of xanthan microgels.[50] Morris et al.[50] showed that microgels appear to consist of a side-by-side association of xanthan macromolecules. Also, Wissenburg et al.[49] have observed the apparition of DNA aggregates in semidilute regime which appear to form loose associations. Also, note that long-range attractive forces between polyions have been postulated recently.[52,53]

5. Conclusion

We have presented the results of the light scattering study of semirigid hyaluronan ($L_0 \approx 100$ Å) and rigid

xanthan ($L_0 \approx 1000$ Å) in dilute and semidilute good solvent solutions. In dilute regime, typical good solvent behavior is found, and the intrinsic persistence length L_0 of hyaluronan and xanthan was determined using a wormlike chain model (Figure 2). However, in the semidilute regime, the time autocorrelation function of the scattered electric field measured by dynamic light scattering is found to be bimodal (Figure 5). The short time relaxation has a typical q^{-2} dependence (Figure 6) and is attributed to the relaxation of concentration fluctuations characterized by a cooperative diffusion mechanism (Figure 9). For the high hyaluronan molecular weight samples and xanthan samples, the long time relaxation has a q^{-3} dependence (Figure 6), characteristic of intraparticle dynamics. For low hyaluronan molecular weight samples, the long time relaxation has a q^{-2} dependence.

The slow mode could be due to the self-diffusion of hyaluronan and xanthan association complexes in the overlapped network. However, the nature of these associations in good solvent semidilute solutions still remain an open discussion. The results show that aggregation of semirigid and rigid chains occurs for hyaluronan and xanthan in excess salt good solvent solutions, where the charged groups of the polyelectrolyte are screened by the salt ions. Associations seem to be a general feature of many charged semirigid and rigid polysaccharides and natural polymers. Also, we think the high rigidity of these natural polymers could be related to the origin of some state of physical associations.

References and Notes

(1) Odijk, T. *J. Polym. Sci., Polym. Phys.* **1977**, *15*, 477.
(2) Skolnick, J.; Fixman, M. *Macromolecules* **1977**, *10*, 944.
(3) Fixman, M. *J. Chem. Phys.* **1982**, *76*, 6346.
(4) Le Bret, M. *J. Chem. Phys.* **1982**, *76*, 6243.
(5) Manning, G. S. *J. Chem. Phys.* **1969**, *51*, 924.
(6) Schmitz, K. S.; Lu, M.; Gauntt, J. *J. Chem. Phys.* **1983**, *78*, 5059.
(7) Schmitz, K. S.; Yu, J. *Macromolecules* **1988**, *21*, 484.
(8) Förster, S.; Schmidt, M.; Antonietti, M. *Polymer* **1990**, *31*, 781.
(9) Sedlák, M.; Amis, E. J. *J. Chem. Phys.* **1992**, *96*, 817.
(10) Ermi, B. D.; Amis, E. J. *Macromolecules* **1996**, *29*, 2703.
(11) Ermi, B. D.; Amis, E. J. *Macromolecules* **1998**, *31*, 7378.
(12) Reed, W. F. *Macromolecules* **1994**, *27*, 873.
(13) Rinaudo, M. *J. Appl. Polym. Sci.: Appl. Polym. Symp.* **1993**, *52*, 11.
(14) Gamini, A.; de Bleijser, J.; Leyte, J. C. *Carbohydr. Res.* **1991**, *220*, 33.
(15) Stokke, B. T.; Elgsaeter, A.; Smidsrød, O. *Int. J. Biol. Macromol.* **1986**, *8*, 217.
(16) Cummins, H. Z.; Pike, E. R. *Photon Correlation and Light Beating Spectroscopy;* Plenum Press: New York, 1974.
(17) Koppel, D. E. *J. Chem. Phys.* **1972**, *57*, 4814.
(18) Provencher, S. W. *Makromol. Chem.* **1985**, *82*, 632.
(19) Coviello, T.; Burchard, W.; Dentini, M.; Crescenzi, V. *Macromolecules* **1987**, *20*, 1102.
(20) De Gennes, P. G. *Scaling Concepts in Polymer Physics;* Cornell University Press: Ithaca, NY, 1979.
(21) Fetters, L. J.; Hadjichristidis, H.; Lindner, J. S.; Mays, J. W. *J. Phys. Chem.* **1994**, *23*, 619.
(22) Benoît, H.; Doty, P. *J. Phys. Chem.* **1953**, *57*, 958.
(23) Buhler, E.; Boué, F. Private Communication, Small Angle Neutron Scattering experiments performed in Saclay, France, 2001.
(24) Glatter, O.; Kratky, O. *Small-Angle X-ray Scattering*; Academic Press: London, 1982.
(25) Sharp, P.; Bloomfield, V. A. *Biopolymers* **1968**, *6*, 1201.
(26) Brûlet, A.; Boué, F.; Cotton, J. P. *J. Phys. II* **1996**, *6*, 885.
(27) des Cloizeaux, J. *Macromolecules* **1973**, *6*, 403.
(28) Coviello, T.; Kajiwara, K.; Burchard, W.; Dentini, M.; Crescenzi, V. *Macromolecules* **1986**, *19*, 2826.
(29) Schmidt, M.; Paradossi, G.; Burchard, W. *Makromol. Chem., Rapid Commun.* **1985**, *6*, 767−772.
(30) Paradossi, G.; Brant, D. A. *Macromolecules* **1982**, *15*, 874−879.
(31) Sato, T.; Norisuye, T.; Fujita, H. *Macromolecules* **1984**, *17*, 2696−2700.
(32) Adam, M.; Delsanti, M. *J. Phys., Lett.* **1977**, *38*, L-271.
(33) Dubois-Violette, E.; de Gennes, P. G. *Physics* **1967**, *3*, 181.
(34) Raspaud, E.; Lairez, D.; Adam, M.; Carton, J. P. *Macromolecules* **1994**, *27*, 2956.
(35) Akcasu, A. Z.; Benmouna, M.; Han, C. C. *Polymer* **1980**, *21*, 866.
(36) Tanahatoe, J. J.; Kuil, M. E. *J. Phys. Chem. B* **1997**, *101*, 9233.
(37) Tanahatoe, J. J.; Kuil, M. E. *J. Phys. Chem. B* **1997**, *101*, 10839.
(38) Klucker, R.; Munch, J. P.; Schosseler, F. *Macromolecules* **1997**, *30*, 3839.
(39) Esquenet, C.; Buhler, E. *Macromolecules* **2001**, *34*, 5287.
(40) Buhler, E.; Munch, J. P.; Candau, S. J. *J. Phys. II* **1995**, *5*, 765.
(41) Adam, M.; Delsanti, M. *Macromolecules* **1985**, *18*, 1760.
(42) Brochard, F.; de Gennes, P. G. *Macromolecules* **1977**, *10*, 1157.
(43) Semenov, A. N. *Physica A* **1990**, *166*, 263.
(44) Doi, M.; Onuki, A. *J. Phys. II* **1992**, *2*, 1631.
(45) Wang, C. H. *Macromolecules* **1992**, *25*, 1524.
(46) Sun, T.; King, H. E. *Macromolecules* **1996**, *29*, 3175.
(47) Buhler, E.; Rinaudo, M. *Macromolecules* **2000**, *33*, 2098.
(48) Schulz, L.; Burchard, W.; Dönges, R. In *Cellulose Derivatives. Modification, Characterization and Nanostructures*; Heinze, T. J., Glasser, W. G., Eds.; ACS Symposium Series 688; American Chemical Society: Washington, DC, 1998; Chapter 16.
(49) Wissenburg, P.; Odijk, T.; Cirkel, P.; Mandel, M. *Macromolecules* **1995**, *28*, 2315.
(50) Morris, V. J.; Franklin, D.; I'Anson, K. *Carbohydr. Res.* **1983**, *121*, 13.
(51) Coviello, T.; Burchard, W.; Geissler, E.; Maier, D. *Macromolecules* **1997**, *30*, 2008.
(52) Odijk, T. *Macromolecules* **1994**, *27*, 4998.
(53) Ray, J.; Manning, G. S. *Langmuir* **1994**, *10*, 2450.

MA012047Q